JGP Journal of General Physiology

RESEARCH ARTICLE

The N terminus of α-ENaC mediates ENaC cleavage and activation by furin

Pradeep Kota[1], Martina Gentzsch[1,2], Yan L. Dang[1], Richard C. Boucher[1], and M. Jackson Stutts[1]

Epithelial Na^+ channels comprise three homologous subunits (α, β, and γ) that are regulated by alternative splicing and proteolytic cleavage. Here, we determine the basis of the reduced Na^+ current (I_{Na}) that results from expression of a previously identified, naturally occurring splice variant of the α subunit (α-ENaC), in which residues 34–82 are deleted ($\alpha_{\Delta 34-82}$). $\alpha_{\Delta 34-82}$-ENaC expression with WT β and γ subunits in *Xenopus* oocytes produces reduced basal I_{Na}, which can largely be recovered by exogenous trypsin. With this $\alpha_{\Delta 34-82}$-containing ENaC, both α and γ subunits display decreased cleavage fragments, consistent with reduced processing by furin or furin-like convertases. Data using MTSET modification of a cysteine, introduced into the degenerin locus in β-ENaC, suggest that the reduced I_{Na} of $\alpha_{\Delta 34-82}$-ENaC arises from an increased population of uncleaved, near-silent ENaC, rather than from a reduced open probability spread uniformly across all channels. After treatment with brefeldin A to disrupt anterograde trafficking of channel subunits, I_{Na} in oocytes expressing $\alpha_{\Delta 34-82}$-ENaC is reestablished more slowly than that in oocytes expressing WT ENaC. Overnight or acute incubation of oocytes expressing WT ENaC in the pore blocker amiloride increases basal ENaC proteolytic stimulation, consistent with relief of Na^+ feedback inhibition. These responses are reduced in oocytes expressing $\alpha_{\Delta 34-82}$-ENaC. We conclude that the α-ENaC N terminus mediates interactions that govern the delivery of cleaved and uncleaved ENaC populations to the oocyte membrane.

Introduction

Epithelial Na^+ channel (ENaC), the highly selective ion channel that conducts Na^+ across the apical membrane of many epithelia, is a heterooligomer composed of homologous α, β, and γ subunits (Canessa et al., 1994b; Garty and Palmer, 1997). Each subunit spans the plasma membrane twice and projects intracellular N and C termini of 50–90 residues and a large disulfide interlinked extracellular domain (Canessa et al., 1994a). Proteolytic cleavage at defined sites in the extracellular domains of α- and γ-ENaC strongly increases ENaC open probability (P_O; Kleyman et al., 2009). In a phenomenon called Na^+ feedback inhibition, increased intracellular Na^+ activity diminishes the extent of ENaC cleavage and P_O, which reduces Na^+ entry into the cell (Anantharam et al., 2006; Knight et al., 2008; Patel et al., 2013, 2014). In the simplest case, this homeostatic regulation of intracellular Na^+ activity controls the magnitude of epithelial Na^+ absorption and potentially influences other cellular processes affected by intracellular Na^+ activity (Ruan et al., 2012; Awayda, 2016). Recent work links the potential physiologic role of Na^+ feedback inhibition to cleavage of ENaC during its processing to the cell surface (Patel et al., 2014; Heidrich et al., 2015). The Frindt and Palmer (2015) and Myerburg et al. (2006) groups showed that increasing intracellular Na^+ decreases the ENaC cleavage that could be ascribed to furin-like convertases. In addition, these laboratories found that increased intracellular Na^+ decreased complex maturation of ENaC N-glycans, a process that occurs during transit through the Golgi compartment. In contrast to detailed mechanisms proposed to mediate retrograde trafficking of ENaC (Butterworth, 2010; Soundararajan et al., 2012), current knowledge of ENaC forward processing does not identify candidate steps or processes for regulation of ENaC function.

Hughey et al. (2003, 2004a) first reported furin mediated cleavage and stimulation of ENaC and, subsequently, identified two distinct populations of ENaC at the cell surface. One population, cleaved at all furin sites, displayed complex glycans, whereas the second population had not undergone posttranslational modification (Hughey et al., 2004b). The characteristics of these populations parallel the differences in cleavage and glycan maturation seen in ENaC produced under conditions of low and high intracellular Na^+ activity, respectively (Patel et al., 2013; Heidrich et al., 2015). Thus, the cellular processes invoked in Na^+ feedback inhibition modify the balance between cleaved and uncleaved ENaC populations at the cell surface. Conceptually, this could be achieved by a Na^+-sensitive branch point in ENaC trafficking that directs ENaC away from compartments

[1]Marsico Lung Institute, Cystic Fibrosis Center and Department of Medicine, University of North Carolina, Chapel Hill, NC; [2]Department of Cell Biology and Physiology, University of North Carolina, Chapel Hill, NC.

Correspondence to M. Jackson Stutts: jack_stutts@med.unc.edu.

that contain furin- and glycan-modifying enzymes. This possibility fits with an area of research known as "unconventional" or "Golgi bypass" trafficking, in which membrane proteins reach their destination without Golgi–trans-Golgi network (TGN) transit (Tveit et al., 2009; Grieve and Rabouille, 2011). Alternatively, factors inherent to ENaC itself, such as extracellular domain conformation may influence the extent of posttranslational modifications. For example, we previously reported that mutation of the lysine clusters in the N terminus of γ-ENaC prevented efficient cleavage of extracellular domains of α and γ subunits in ENaC delivered to the membrane (Kota et al., 2014). Additionally, ubiquitinylation of ENaC, which modifies N-terminal lysines, decreased the cleavage of ENaC at the cell surface (Ruffieux-Daidié et al., 2008; Ruffieux-Daidié and Staub, 2011). Each of these studies implicated ENaC's cytosolic termini in allosteric control of cleavage occurring in ENaC extracellular domains, although neither study ruled out contributions of ENaC trafficking to the observed results.

Our interest in the ability of ENaC cytosolic termini to influence ENaC cleavage/activation led us to revisit a study by Chraïbi et al. (2001) on a naturally occurring splice variant of the N terminus of mouse kidney α-ENaC, which produced ENaC with low P_O. Here, we report that the spliced-out segment of the α-ENaC N terminus ($\Delta_{34–82}$) described in the earlier study contains residues that strongly influence cleavage at sites in the extracellular domains of ENaC heterooligomers. Importantly, the spliced-out segment of the α-ENaC N terminus includes residues that are essential for regulation of ENaC through Na^+ feedback inhibition.

Materials and methods

Constructs and mutagenesis

Rat ENaC subunits were cloned into pSDE vector, and deletion of α-ENaC N-terminal residues was performed using standard PCR-based cloning approaches. Mutants were generated using site-directed mutagenesis of full-length α-ENaC construct. Mutations were confirmed by sequencing.

Oocyte injections and electrophysiology

Our previous studies contain detailed methods for expression and analysis of ENaC in *Xenopus* oocytes (Garcia-Caballero et al., 2008; Gentzsch et al., 2010; Kota et al., 2012). Female *Xenopus* were housed and used according to protocols and with the supervision of the University of North Carolina Institutional Animal Care and Use Committee. Stage V–VI oocytes were isolated surgically and injected with complementary RNAs (cRNAs) encoding α-, β-, and γ-ENaC subunits (0.15 or 0.3 ng each) only or in combination with human furin or matriptase (1.0 ng each). Depending on the study objective, we injected α- or γ-ENaC cRNA double tagged with hemagglutinin (HA) and V5 epitopes at the N and C termini, respectively. To label γ-ENaC at the surface, we engineered a cysteine at residue 133 and exposed expressing oocytes to fluorescently tagged *N*-methyl maleimide. To express ENaC, we incubated injected oocytes in Barth medium for 24 h before study. For some experiments, amiloride was included in the overnight incubation at 10 µM final concentration. We recorded ENaC current (I_{Na}) as amiloride-sensitive, two-electrode voltage-clamp current. To stimulate basal I_{Na}, we added trypsin or chymotrypsin directly to the perfusion chamber at 4–10 µg/ml final concentration. To estimate ENaC whole-cell P_O (WCP_O), we replaced WT β-ENaC with β_{S518C}-ENaC (Snyder et al., 2000; Kellenberger et al., 2002). The sulfhydryl reagent MTSET covalently binds the engineered cysteine of open channels, causing the channel to be locked open with a P_O near unity and 30% reduced single-channel conductance. The ratio of I_{Na} recorded before and after MTSET exposure (adjusted for conductance) yielded an estimate of WCP_O.

Western blotting

We prepared lysates from oocytes as described by García-Caballero et al. (2008). After separation by 7–10 or 4–20% SDS-PAGE, proteins were transferred to nitrocellulose. HA-tagged and V5-tagged α- and γ-ENaC were recognized with an anti–HA mAb (clone HA.11; Covance) and an anti–V5 mAb (Invitrogen), respectively.

Maleimide labeling

24 h after injection of cRNA (0.3 ng each of α-, β-, and γ-ENaC subunits), oocytes were labeled with 40 µM IRDye 680RD Maleimide (LI-COR) in Modified Barth Saline (MBS) buffer for 1 h at 4°C. Labeling was quenched with 10 mM cysteine, and oocytes were washed extensively with MBS supplemented with cysteine followed by MBS without cysteine. Lysates from oocytes were prepared as described previously (Gentzsch et al., 2010). Immunoprecipitations of proteins from lysates were performed in Nonidet P-40 buffer (Cholon et al., 2010) followed by incubation with Protein A/G agarose (Santa Cruz Biotechnology). Eluates were processed for Western blotting as described above.

Brefeldin A (BFA) experiments

In one series of experiments, BFA (3 µM) or vehicle (DMSO) was included with the overnight incubation–medium oocytes injected with WT ENaC or ENaC that contained $\alpha\Delta_{34–82}$-ENaC. After overnight incubation, these groups were moved into fresh Barth medium, and basal and stimulated I_{Na} were recorded at 0, 2, and 6 h. In a second series of experiments with the same injection groups, BFA (µM) or vehicle (DMSO) was introduced after overnight incubation in Barth medium, and basal and stimulated I_{Na} were recorded 5 h later.

Analysis

The densitometry of Western blot bands associated with ENaC fragments was performed with gel-analysis software in ImageJ (National Institutes of Health). Basal and stimulated I_{Na} are reported as means ± SEM. Statistical analyses were applied as indicated through the Prism 6 graphics software suite (GraphPad Software, Inc.).

Results

Chraïbi et al. (2001) identified a natural splice variant of α-ENaC in RNA isolated from mouse kidney, which predicted deletion of residues 34–82 of the 108 residues in the cytosolic N terminus (ΔNT). They reported that the α-ENaC ΔNT produced a lower

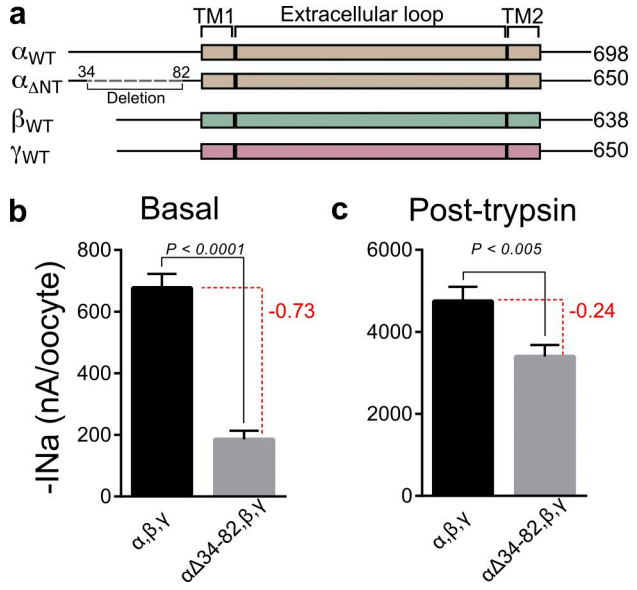

Figure 1. **Deletion of residues 34–82 of α-ENaC reduces ENaC current. (a)** Topologic representations of rat α-, β-, and γ-ENaC subunits. The α-ENaC splice variant with the missing residues is shown as dashed lines. **(b and c)** WT or splice variant α-ENaC cRNA was injected into *Xenopus* oocytes with WT β- and γ-ENaC. Amiloride-inhibited current (I_{Na}) was recorded 20–24 h after injection. Trypsin (2.0 µg/ml) was added during continuous recording. n = 15 separate oocytes collected from three donor frogs. Mean basal I_{Na} (b) decreased by 73% and trypsin-stimulated I_{Na} (c) decreased by 24%, compared by Student's t test. Error bars represent mean ± SEM.

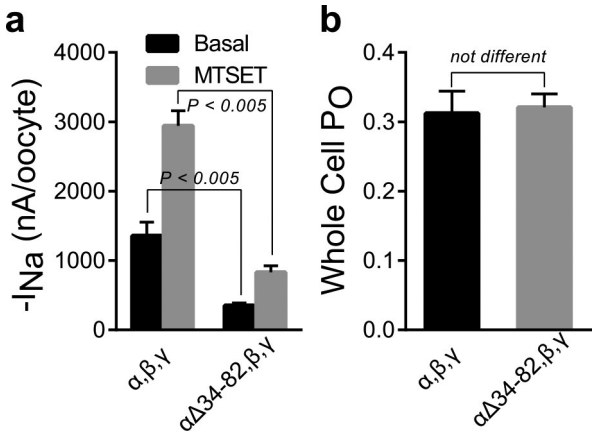

Figure 2. **WCP_O is unaffected by α-ENaC N-terminal splice deletion. (a)** Oocytes injected with ENaC subunits as in Fig. 1, except that β-$ENaC_{S518C}$ replaced the WT β-ENaC RNA. After recording of basal I_{Na}, oocytes were exposed to 1 mM MTSET and two-electrode voltage clamp current recording continued for 3–5 min. **(b)** WCP_O was calculated using the data from panel a (see Materials and methods). n = 20 (WT) or n = 21 (splice variant) oocytes from four frogs, two-way ANOVA. Error bars represent mean ± SEM.

amiloride-sensitive current (I_{Na}) when expressed in oocytes with WT β- and γ-ENaC. We compared the I_{Na} generated by ENaC containing rat WT or ΔNT α-ENaC in *Xenopus* oocytes and found a 73% reduction in basal I_{Na}, as reported by Chraïbi et al. (2001); (Fig. 1 a). Chraïbi et al. (2001) further observed 28% reduced surface expression of the splice variant compared with WT. Based on the observation that the single channel conductance of this variant was similar to that of WT ENaC, Chraïbi et al. (2001) deduced that P_O is a component of the reduced basal current. As a focus of our work has been proteolytic stimulation of ENaC P_O, we included a 5-min exposure to trypsin in our recording protocols. Externally applied trypsin fully cleaves ENaC present at the cell surface, producing a P_O ≥0.7 (Caldwell et al., 2004). Trypsin-stimulated I_{Na} is, therefore, proportional to, and a reliable readout for, surface expression. Upon exposure to trypsin, both WT and αΔNT coexpressed with WT β- and γ-ENaC responded with increased I_{Na}. Interestingly, the splice variant ENaC had a proportionally greater increase in I_{Na} resulting in trypsin-stimulated I_{Na} that was only 24% reduced compared with WT ENaC (Fig. 1 b). This reduction is quite consistent with the modestly diminished surface expression of the variant reported in the earlier study (Chraïbi et al., 2001).

The sulfhydryl reagent MTSET covalently bonds the engineered cysteine in the β-ENaC mutant β_{S518C} of ENaC oligomers in the open conformation and sterically prevents channel closure (Sheng et al., 2001; Kellenberger et al., 2002; Anantharam et al., 2006; Winarski et al., 2010). To determine whether ENaC containing αΔNT expresses decreased P_O, as concluded previously, we recorded the MTSET responses of ENaC with βS518C, WT γ-ENaC, and WT or ΔNT α-ENaC (Fig. 2; Chraïbi et al., 2001). Consistent with our earlier observations, basal I_{Na} of ΔNT ENaC was reduced compared with that of WT ENaC (Fig. 1). Furthermore, stimulation with MTSET did not result in a proportionately larger increase in basal I_{Na} of ENaC oligomers containing ΔNT compared with those with WT α-ENaC. Therefore, N-terminal deletion in α-ENaC does not generate ENaC on the oocyte surface with uniformly reduced P_O. Indeed, WCP_O calculated after exposure to MTSET (Fig. 2 a) for ΔNT ENaC was not significantly different from WT WCP_O (Fig. 2 b). The basis for this unanticipated result proved helpful to understanding the effect of deleting residues in the α-ENaC N terminus on ENaC function.

MTSET forms a covalent bond to the engineered cysteine at the degenerin residue in β-ENaC (Snyder et al., 2000; Kellenberger et al., 2002). Reaction occurs when channel opening exposes the engineered cysteine and prevents closure of the open channel. However, channels that do not open, or that open only briefly, are unaffected by MTSET. Such channels, which have been described as "near silent," are susceptible to proteolytic stimulation (Caldwell et al., 2004, 2005). The data in Fig. 1, showing substantial stimulation of ΔNT ENaC by trypsin, and the data in Fig. 2, showing resistance of ΔNT ENaC to MTSET, can be reconciled if the presence of ΔNT α-ENaC increases the proportion of near-silent ENaC oligomers populating the oocyte surface. We tested this possibility in experiments summarized in Fig. 3. As shown in Fig. 3 a, after METSET exposure, trypsin briskly stimulated I_{Na} of both WT and αΔNT ENaC. This indicates that both WT and αΔNT ENaC produce a population of near-silent channels on the oocyte surface that do not respond to MTSET. The results of this protocol are summarized in Fig. 3 b. The apparent WCP_O derived from basal and MTSET-stimulated I_{Na} was not different in WT and mutant groups (WT = 0.24 ± 0.025; αΔNT, β, and γ = 0.26 ± 0.025; n = 14/group). However, from the trypsin increment of steady-state, MTSET-stimulated I_{Na}, we estimate 90% of the channels on the surface of αΔNT ENaC-expressing

oocytes to fit the near-silent definition. In contrast, the fraction of WT ENaC deemed near silent was ~65%. The data summarized in Fig. 3 c indicate that both WT and αΔNT ENaC treated with trypsin exhibit stimulated I_{Na} that is not modified by MTSET. With stimulated I_{Na}, no increment with MTSET indicated a WCP_O of ~0.7, consistent with previous single-channel measurements.

To understand the apparent, diminished proteolytic activation of ENaC containing αΔNT, we performed Western blot analysis of ENaC proteolytic fragments. Others have reported the critical importance of γ-ENaC cleavage in proteolytic stimulation of ENaC (Diakov et al., 2008). I_{Na} from ENaC-expressing oocytes correlates with the presence of a faster-migrating band in Western blots, representing the form of γ-ENaC that has been cleaved either during anterograde trafficking to the cell surface or by the action of surface-resident proteases. To evaluate the extent to which γ-ENaC is proteolyzed in the presence of αΔNT ENaC, we isolated crude membranes from oocytes and solubilized ENaC, as described in Materials and methods. In oocytes expressing WT or αΔNT-ENaC, a significant amount of γ-ENaC coexpressed with WT β-ENaC appeared as faster migrating species, representative of the C-terminal fragment predicted to arise from furin cleavage (Fig. 4 a). Strikingly, this furin fragment was significantly diminished when WT β and γ subunits were expressed with αΔNT-ENaC (Fig. 4 a). Given the recognized important contribution of γ-ENaC cleavage to ENaC P_O, this result is clearly consistent with the low basal I_{Na} of ENaC containing αΔNT ENaC.

Furin or furin-like convertases also cleave α-ENaC during ENaC anterograde transport to the cell surface. During SDS-PAGE, full-length αΔNT-ENaC migrated more rapidly than WT α-ENaC did, consistent with deletion of 48 residues from the N terminus (Fig. 4 b). In contrast to the significant reduction in basal γ-ENaC cleavage seen with αΔNT ENaC, the fragment associated with furin cleavage of αΔNT ENaC appeared little different from WT α-ENaC under basal conditions (Fig. 4 b, compare the WT and ΔNT lanes). To probe that result further, we coexpressed furin with WT and αΔNT ENaC (Fig. 4 b). Furin coexpression increased the density of the band, consistent with furin-mediated cleavage of WT α-ENaC, and increased the proportion of total WT α-ENaC appearing as the furin fragment. With use of the C-terminal V5 epitope, the furin fragment from αΔNT-ENaC migrates in the same manner as the furin fragment of WT α-ENaC. Importantly, furin coexpression did not increase the ratio of furin fragment to full-length αΔNT-ENaC. Thus, the residues deleted from the α-NT are important for cleavage of both α- and γ-ENaC furin sites.

We also verified that the α-NT deletion reduced cleavage of γ-ENaC expressed on the surface (Fig. 4 c). For that purpose, we developed a sensitive method of surface labeling by inserting an engineered cysteine at residue 133 of rat γ-ENaC, preceding the 135–138RRKR furin site. Maleimide efficiently labeled ENaC with γ-ENaC 133C but not WT γ-ENaC. We observed a small fraction of total γ-ENaC as full length at the surface, when paired with WT α- and β-ENaC. Coexpressed furin eliminated this species, consistent with cleavage of FL γ-ENaC. When expressed with αΔNT-ENaC and WT β-ENaC, full-length γ-ENaC 133C was strongly labeled by maleimide. Moreover, full-length γ-ENaC surface expression persisted with coexpressed furin if ENaC oligomers

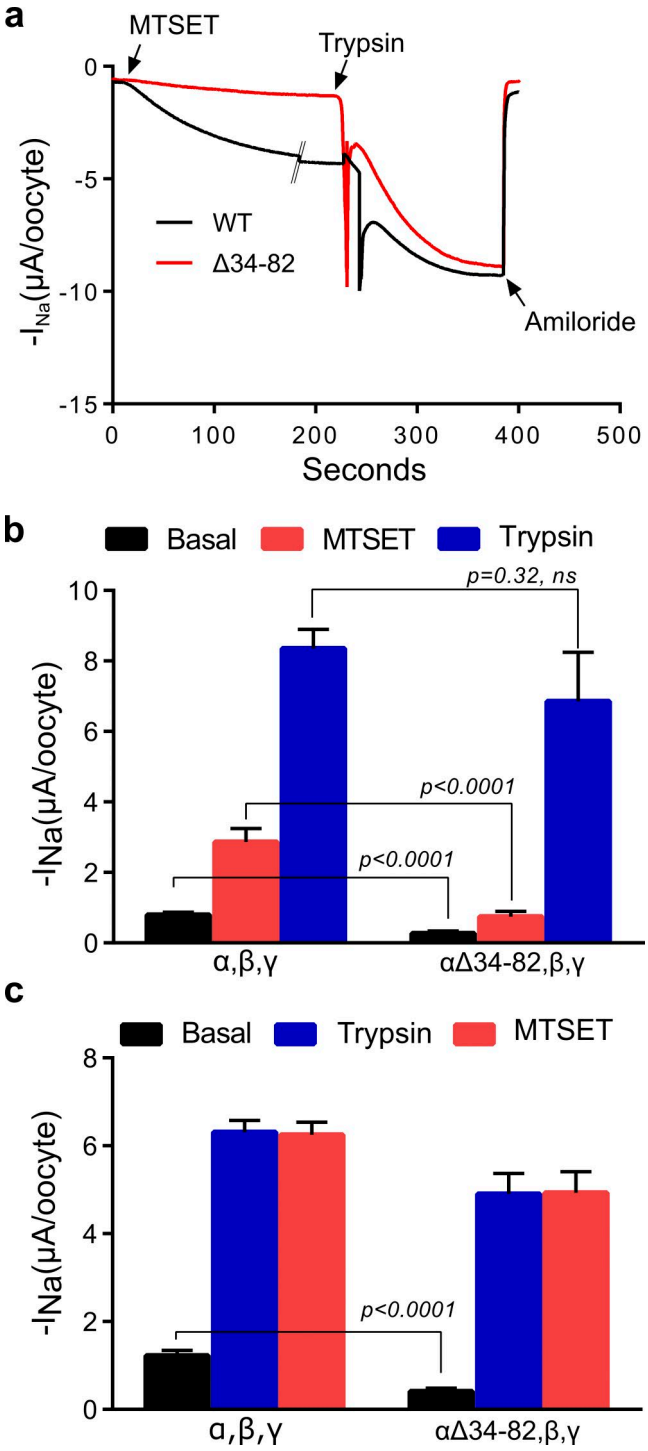

Figure 3. **Trypsin overcomes $\alpha_{\Delta 34-82}$-ENaC resistance to MTSET.** Oocytes injected with ENaC subunits, as in Fig. 2, with β-$ENaC_{S518C}$ replacing the WT β-ENaC RNA. **(a)** Representative two-electrode voltage clamp current traces illustrating WT (black trace) and $\alpha_{\Delta 34-82}$-ENaC (red trace) response to MTSET, followed by trypsin. **(b)** Summary data from the previous panel (a). *n* = 14 oocytes/group from three frogs. **(c)** After trypsin, $\alpha_{\Delta 34-82}$-, β-, and γ-ENaC was not resistant to MTSET. Similar experiment as in the other two panels (a and b), but trypsin exposure preceded MTSET. *n* = 6/group. Error bars represent mean ± SEM.

contained αΔNT-ENaC. Thus, deletion of residues 34–82 in the α-ENaC N-terminus prevents furin-mediated cleavage of FL

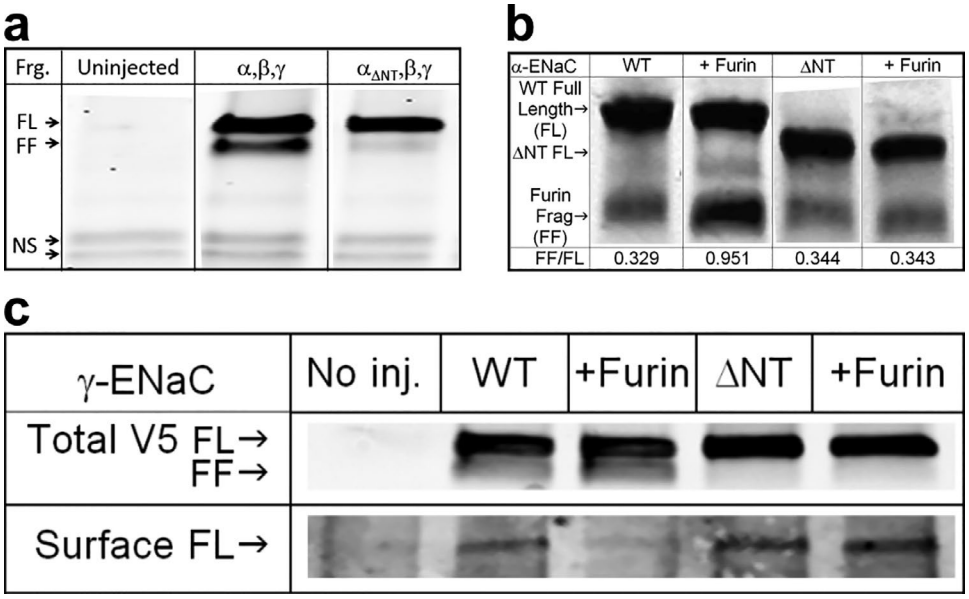

Figure 4. **The splice variant $\alpha\Delta_{NT}$ reduces γ-ENaC furin site cleavage. (a)** Crude membrane samples of uninjected oocytes or oocytes injected with WT or Δ_{NT} α-ENaC plus WT β-ENaC and HA/V5 epitope-tagged γ-ENaC were prepared as described in Materials and methods and subjected to PAGE and blotted for the V5 epitope tag. In WT α-, β-, and γ-ENaC, samples appeared as a band consistent with full-length (FL) γ-ENaC and a more rapidly migrating band predictive of cleavage at the γ-ENaC furin site (FF). Deletion of N-terminal residues of α-ENaC sharply diminished FF staining in total and as a fraction of FL. All lysates generated a doublet unrelated to ENaC (NS). This result is representative of multiple similar experiments. **(b)** WT or Δ_{NT} α-ENaC was injected, along with WT β-ENaC and γ-ENaC, to comprise two experimental groups of 60 oocytes each. One-half of each group was also injected with furin RNA (1.0 ng/oocyte). α-ENaCs were V5 epitope tagged at the C terminus. Samples were processed and analyzed as in the previous panel (a). Full-length Δ_{NT} α-ENaC (labeled ΔNT FL) migrated faster than WT FL, as expected. Fragments consistent with furin cleavage—furin frag (FF)—migrated identically, as expected for C-terminal V5-tagged fragments. The fraction of FF/FL in each condition was obtained from densitometry and is indicated beneath each lane. Similar results were obtained in other trials. **(c)** We mutated residue 133E of γ-$ENaC_{HA/V5}$ to 133C and coexpressed the mutant with WT β-ENaC and WT or ΔNT α-ENaC. After 24 h, oocytes were labeled with 40 µM Alexa Fluor 680 C2 maleimide in MBS^{++} buffer. Labeling was quenched with 10 mM cysteine, and oocytes were washed extensively. Western blots of total lysates, stained for the V5 epitope tag (Total) or for γ-ENaC labeled by fluorescent maleimide (Surface) are shown. Representative of multiple similar experiments.

γ-ENaC. The presence of FL γ-ENaC at the cell surface and its persistence in the face of coexpressed furin are consistent with reduced basal I_{Na} generated by αΔNT-ENaC, and they predict reduced stimulation of I_{Na} by furin (see below).

To further understand how deleting α-ENaC residues 34–82 blunted ENaC proteolysis, we compared cleavage and stimulation of αΔNT ENaC by furin and matriptase (Fig. 5). Matriptase exerts its trypsin-like activity at the cell surface, and we found (Kota et al., 2012, 2014) that matriptase fully stimulated ENaC when coexpressed in oocytes, i.e., exogenous trypsin exerted no further stimulation. For WT ENaC, furin coexpression increased the proportion of the species representing the γ-ENaC furin fragment (Fig. 5 a, see legend). Coexpressed matriptase converted most of the full-length and furin-fragment γ-ENaC to faster migrating species, consistent with matriptase cleavage at ∼40 residues downstream from the furin site. As seen above, γ-ENaC, as a part of αΔNT ENaC oligomers, displayed little furin fragment, and coexpressed furin caused only a small increase in the furin-fragment band intensity. However, for WT ENaC, coexpressed matriptase converted most γ-ENaC staining to a band consistent with cleavage at downstream, secondary cleavage sites. Functional results reflect these biochemical findings. Furin stimulation of αΔNT ENaC basal I_{Na} was reduced compared with WT ENaC but was recovered with trypsin (Fig. 5, b and c). Matriptase expression substantially stimulated basal I_{Na}, irrespective of the αENaC subunit, although the stimulation of the splice variant was not as robust as that of WT (Fig. 5, d and e). We concluded that residues 34–82 of α-ENaC are required for furin-mediated cleavage and stimulation of ENaC but are not essential for cleavage by coexpressed matriptase.

Inhibition of ENaC proteolytic processing has been implicated in Na^+ feedback inhibition (Anantharam et al., 2006; Knight et al., 2008; Patel et al., 2014). We asked whether the influence of the α-ENaC N terminus that we detected upon ENaC cleavage related to that mode of ENaC regulation. Cultures of mammalian cells expressing ENaC, with and without amiloride, have become a standard maneuver for the study of Na^+ self-inhibition by creating relatively modest differences in intracellular Na^+ activity (Heidrich et al., 2015). Knight et al. (2008) showed amiloride-induced effects on ENaC cleavage were mediated by intracellular Na^+. After 24 h expression of WT or αΔNT-ENaC in Barth medium ($[Na^+]$ = 96 mM), we recorded basal and stimulated I_{Na} of WT or αΔNT-ENaC oocytes and exposed others of each group to 10 µM amiloride for 6 h. In the WT group, basal I_{Na} increased dramatically, whereas I_{Na} of the $\alpha\Delta_{34-82}$-ENaC group was unchanged (Fig. 6 a). In oocytes expressing ENaC, it is common practice to increase the level of ENaC current expressed by overnight incubation in amiloride after cRNA injection. Indeed, incubation in amiloride during the 24-h period after cRNA injection produced larger I_{Na} in oocytes expressing WT ENaC (Fig. 6 b). In contrast,

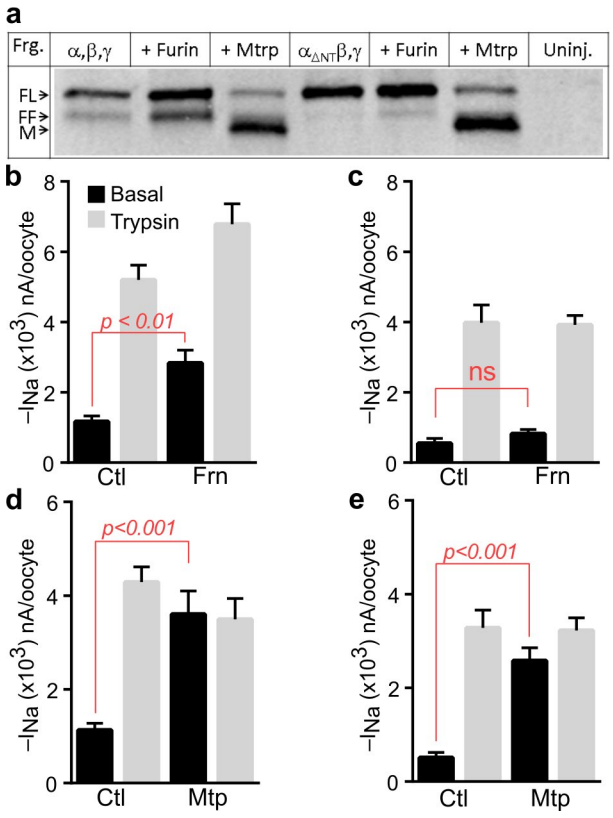

Figure 5. **Residues 34–82 of α-NT are not required for γ-ENaC cleavage by matriptase. (a)** Oocyte membrane samples prepared as in Fig. 4 were blotted for γ-ENaC (C-terminal V5 epitope tag) expressed with WT α- and β-subunits (three leftmost lanes) or $\alpha_{\Delta NT}$- and WT β-subunits (next three lanes to the right). ENaC groups were coinjected with furin or matriptase (Mtrp.). Labeled bands identify γ-ENaC as full length (FL), furin fragment (FF), and matriptase fragment (M). **(b–e)** Stimulation of I_{Na} by coexpressed furin (WT ENaC; b), ($\alpha_{\Delta NT}$-ENaC; c), or by coexpressed matriptase (WT ENaC; d), ($\alpha_{\Delta NT}$-ENaC; e). After recording basal I_{Na} (black bars), recording continued in the presence of 2 µg/ml. Current in each condition was normalized to stimulated I_{Na} in the control group. Error bars are mean ± SEM (10–15 recordings/group from two or three oocyte batches/condition).

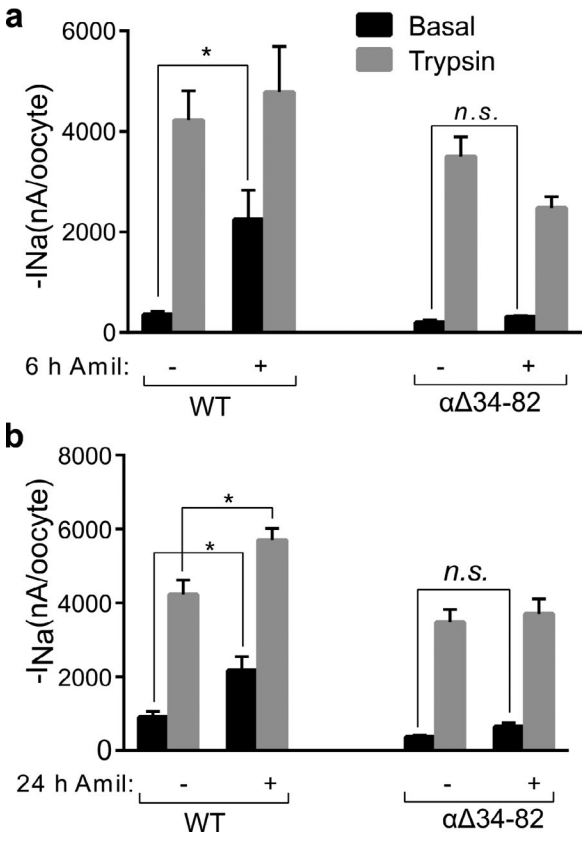

Figure 6. **Amiloride stimulation of I_{Na} is impaired in $\alpha\Delta_{34-82}$-ENaC. (a)** Oocytes injected and incubated in Barth medium for 20 h and recorded as in Fig. 1 (−Amil). Oocytes from each injection group were then incubated in Barth medium with amiloride (10 µM) for 6 h and recorded (+Amil). **(b)** Oocytes were injected as in Fig. 1 and incubated for 24 h in Barth medium with or without 10 mM amiloride. Basal and trypsin-stimulated I_{Na} was recorded as above. Data collected from two to three oocyte batches, n = 6–18 recordings/condition. *, $P < 0.05$ for difference from −Amil by two-way ANOVA. Error bars represent mean ± SEM.

the presence of amiloride during 24 h of expression did not affect the I_{Na} of αΔNT-ENaC. Thus, residues within α-ENaC 34–82 appear to mediate the steps in ENaC proteolytic processing that are accelerated in the presence of amiloride.

Our results and those of Chraïbi et al. (2001) consistently show a moderate decrease in ENaC surface expression. To determine whether that finding indicates a difference in surface delivery or stability of the splice variant, we recorded basal and trypsin-stimulated I_{Na} after the washout or application of BFA. BFA is a fungal metabolite that potently and reversibly blocks trafficking of proteins from the ER to the plasma membrane (Misumi et al., 1986; Lippincott-Schwartz et al., 1989). BFA is often used to block ENaC anterograde trafficking and recycling (Butterworth et al., 2005; Patel et al., 2014). As expected from those observations, the I_{Na} of oocytes moved to fresh medium after overnight incubation in BFA increased over 6 h (Fig. 7, a and b). Both basal and stimulated I_{Na} of oocytes expressing $\alpha_{\Delta NT}$-ENaC recovered from BFA more slowly than the currents of oocytes expressing WT ENaC, although the difference was much more evident for basal I_{Na}. The larger difference in basal I_{Na} recovery reflected the impaired furin-mediated cleavage of the splice variant, but the rate of recovery of the splice variant's stimulated I_{Na} was also reduced, consistent with a modestly slower delivery of the mutant to the oocyte surface. Acute application of BFA inhibited basal and stimulated I_{Na} of both expression groups (Fig. 7c). After 5 h, the extent of I_{Na} decay was identical for WT- and $\alpha_{\Delta NT}$-ENaC–expressing oocytes. The clearly slower recovery from BFA treatment of the mutant, with no obvious difference in its BFA-induced I_{Na} decay, suggests that the deleted residues influence interactions that govern ENaC movement through the biosynthetic pathway to the cell surface.

Discussion

Chraïbi et al. (2001) discovered a splice-deletion variant of the rodent α-ENaC N terminus that produced a small basal ENaC current without an equivalently reduced ENaC surface expression. Using electrophysiologic and biochemical maneuvers, we report that this α-ENaC variant undergoes reduced furin-mediated cleavage of α- and γ-ENaC and, thereby, increases the

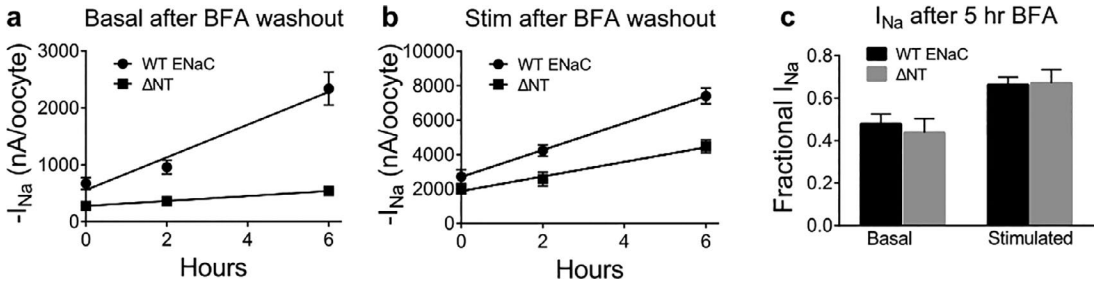

Figure 7. **Slower recovery from BFA exposure by $\alpha_{\Delta NT}$-ENaC. (a and b)** Oocytes injected with WT β- and γ-ENaC subunits with WT or $\alpha_{\Delta NT}$-ENaC were incubated overnight in Barth medium containing 10 µM amiloride and 1 µM BFA. The next day, BFA was removed and basal (a) and simulated (b) I_{Na} was recorded after 2 and 6 h. Basal I_{Na} for WT increased (slope = 287 ± 44 nA/h) more rapidly than for $\alpha_{\Delta NT}$-ENaC (slope = 44 ± 17 nA/h). WT stimulated I_{Na} also increased (slope = 782 ± 91 nA/h) more rapidly than stimulated I_{Na} of $\alpha_{\Delta NT}$-ENaC (slope = 425 ± 84 nA/h). There were 10 oocytes in each injection condition, isolated from two frogs. The slopes and associated errors were generated by linear regression analyses and differ significantly ($P < 0.01$). **(c)** After overnight incubation in Barth medium with 10 µM amiloride, oocytes were exposed to 3 µM BFA or vehicle (DMSO). I_{Na} recorded after 5 h is expressed as fraction of the vehicle control at 5 h (n = 5/injection condition). Error bars represent mean ± SEM.

population of uncleaved ENaC at the oocyte surface. This finding implicates the α-ENaC N terminus in processes and/or interactions that determine the proteolytic status of ENaC delivered to the apical cell membrane of epithelia. Defining the role or roles of α-ENaC N terminus in ENaC proteolytic stimulation in epithelia may reveal how native cells regulate ENaC for distinct physiologic purposes.

Our findings relate to previous work by Hughey et al. (2004b) and Mueller et al. (2007), who identified populations of cleaved and uncleaved ENaC at the cell surface. Only the cleaved population exhibited complex glycans, supporting the notion that ENaC oligomers potentially traffic to the membrane by two routes, one through the Golgi–TGN and the other through an undefined path. Hughey et al. (2004b) and Mueller et al. (2007) presciently speculated that the uncleaved population served as a reservoir of nonconducting ENaC on the cell surface, subject to activation by surface and soluble proteases. In support of that idea, we previously reported (Caldwell et al., 2004) low P_O (near-silent) ENaC, in outside out patches, which became fully active after exposure to trypsin. This two-population model also fits very well with homeostasis of airway-surface liquid by airway epithelial cell cultures, which occurs through regulation of ENaC proteolysis (Myerburg et al., 2006; Tarran et al., 2006). In fact, homeostatic regulation of airway-surface liquid through ENaC proteolysis requires uncleaved ENaC delivered to the cell surface. Moreover, recent studies also link physiologic regulation of ENaC by intracellular Na^+ activity to ENaC cleavage during anterograde trafficking (Patel et al., 2013; Frindt and Palmer, 2015; Heidrich et al., 2015; Frindt et al., 2016). Thus, the timing and cellular location of ENaC cleavage crucially influences how ENaC functions and is regulated in the apical cell membrane of epithelia. Discovery that deletion of α-ENaC residues 34–82 promotes the proportion of uncleaved ENaC oligomers at the surface of oocytes provides clues to better understand this form of ENaC regulation.

The most probable implication of our results involves the α-ENaC N terminus in ENaC anterograde trafficking. During anterograde trafficking, ENaC is subject to furin-mediated endoproteolysis and glycan maturation, two hallmark posttranslational modifications performed within compartments of the Golgi–TGN trafficking route (Hughey et al., 2004b). In theory, this should allow straightforward inference of ENaC's trafficking itinerary under different experimental conditions. Indeed, deleting α-ENaC N terminus residues 34–82 strongly reduced cleavage of ENaC at recognized furin sites. This was evident in both total and tagged surface pools. Our observation that deletion of residues 34–82 is required for ENaC stimulation and cleavage by coexpressed furin, but not by coexpressed matriptase, is consistent with the notion that the N terminus of α-ENaC has a role in trafficking that favors its cleavage during processing to the cell surface. Thus, residues within the α-ENaC N terminus contribute to increasing the proportion of ENaC oligomers expressed on the surface that have undergone furin-mediated cleavage.

Other investigators have examined the importance of the α-ENaC NT on ENaC function. Chalfant et al. (1999) made progressive deletions of the α-ENaC N terminus and identified a stimulatory effect from deletions up to rat α-ENaC residue 67. They attributed this effect to the loss of an endocytic motif. We did not see as dramatic a stimulation of I_{Na} with that deletion. With deletions up to α-ENaC residues 82 and 89, Chalfant et al. (1999) observed inhibition of I_{Na}, similar to what we report here. Mueller et al. (2007) on the other hand, reported that the C terminus of α-ENaC is required for exit from the ER and transit through the Golgi–TGN, with no detectable role for the N terminus in these processes. In their study, the N- or C-terminal domains of α-ENaC were fused to γ-glutamyltranspeptidase or human interleukin receptor α subunit (Tac), respectively. By following maturation of γ-glutamyltranspeptidase and Tac through attained EndoH resistance of N-glycans, the authors found no roles of fused ENaC N termini in exit or retention in the ER. However, proteolytic processing of ENaC was not studied because the intracellular termini of ENaC were studied as chimeras not designed to be cleaved or assemble as functioning channels. Based on the effects of $\alpha\Delta_{34-82}$ on proteolysis of γ-ENaC reported here, the α-ENaC cytosolic N terminus importantly influences furin-mediated processing of ENaC during transit through the Golgi–TGN. Although we did not study ENaC trafficking directly here, in the context of known ENaC processing, we reason that the α-ENaC N terminus has an important role in ENaC processing during anterograde trafficking. This conclusion is strengthened by the slow recovery

of αΔNT ENaC-mediated I_{Na} after washout of BFA (Fig. 7). BFA is frequently used as a tool to identify anterograde trafficking, through its disruption of the Golgi apparatus, and has been specifically applied to the study of ENaC. The much slower recovery of basal I_{Na} compared with stimulated I_{Na} is indicative of the major effect of the deletion on furin-mediated cleavage, with a smaller effect on delivery to the surface.

Na^+ feedback inhibition refers to negative regulation of Na^+ entry by increased intracellular Na^+ activity, a phenomenon recognized to occur in epithelia long before ENaC was identified (Turnheim, 1991). Although multiple mechanisms have been shown to contribute to Na^+ feedback inhibition (Abriel and Horisberger, 1999; Anantharam et al., 2006; Patel et al., 2014), recent studies indicate that increased intracellular Na^+ triggers reduced ENaC cleavage and glycan maturation during anterograde trafficking (Patel et al., 2014; Heidrich et al., 2015). Our observation that α-ENaC residues 34–82 have a role in amiloride stimulation of I_{Na} in ENaC-expressing oocytes relates to observations by Patel et al. (2014). They found that ENaC-expressing oocytes exposed to high salt had reduced surface expression of ENaC and decreased γ-ENaC cleavage. The latter observation, in turn, agrees with other studies that Na^+ feedback inhibition decreases ENaC P_O (Abriel and Horisberger, 1999; Anantharam et al., 2006). Amiloride relieves Na^+ feedback inhibition of ENaC by preventing Na^+ entry. In our studies, amiloride acutely stimulated I_{Na} of WT ENaC but not of ENaC containing an α subunit with deletions or specific mutations of the N terminus. Among potential explanations for this observation, we favor a role for the α-ENaC N terminus in furin-mediated cleavage of γ-ENaC in oocytes. We propose that the α-ENaC N terminus participates in processes or interactions that cause or allow ENaC cleavage during anterograde trafficking and that these interactions or processes may be steps involved in Na^+ feedback inhibition.

In conclusion, we observed dramatic reduction of furin-mediated cleavage of α- and γ-ENaC by deleting α-ENaC residues 34–82. This resulted in an increased population of low P_O ENaC on the oocyte surface, where exogenous protease application fully converted to a high P_O population. Previous studies implicate the balance between low and high P_O populations of surface ENaC in physiologic regulation of apical membrane Na^+ conductance, including by intracellular Na^+ (Patel et al., 2013) and by aldosterone (Frindt and Palmer, 2015). In airway epithelia, homeostasis of airway-surface liquid volume through opposition to ENaC proteolysis requires delivery of uncleaved, low P_O ENaC to the surface (Myerburg et al., 2006; Tarran et al., 2006). The proteolytic status of ENaC delivered to the conducting pool is determined by furin-mediated cleavage during anterograde trafficking, and the presence of cleaved and uncleaved populations of ENaC at the surface indicates that ENaC trafficking to the cell surface may avoid furin-mediated cleavage. Our study of a natural splice variant of rodent α-ENaC identifies the α-ENaC N terminus as mediating interactions that may be involved in essential regulation of epithelial Na^+ absorption. Discovery of the partners in these interactions in future studies should provide a much clearer understanding of ENaC anterograde trafficking used in ENaC regulation and may identify new strategies for manipulating ENaC-mediated Na^+ absorption.

Acknowledgments

This work was supported by the Cystic Fibrosis Foundation and by the National Heart, Lung, and Blood Institute (grant P01 HL110873).

The authors declare no competing financial interests.

Author contributions: P. Kota designed research, analyzed data, and wrote the manuscript. M. Gentzsch conducted research and analyzed data. Y.L. Dang conducted research and analyzed data. R.C. Boucher edited the manuscript. M.J. Stutts designed research, analyzed data, and wrote the manuscript.

Kenton J. Swartz served as editor.

Submitted: 27 July 2017
Revised: 5 March 2018
Accepted: 28 May 2018

References

Abriel, H., and J.D. Horisberger. 1999. Feedback inhibition of rat amiloride-sensitive epithelial sodium channels expressed in Xenopus laevis oocytes. *J. Physiol.* 516:31–43. https://doi.org/10.1111/j.1469-7793.1999.031aa.x

Anantharam, A., Y. Tian, and L.G. Palmer. 2006. Open probability of the epithelial sodium channel is regulated by intracellular sodium. *J. Physiol.* 574:333–347. https://doi.org/10.1113/jphysiol.2006.109173

Awayda, M.S. 2016. Brakes and gas-regulation of ENaC by sodium. *Channels (Austin).* 10:73–74. https://doi.org/10.1080/19336950.2015.1125278

Butterworth, M.B. 2010. Regulation of the epithelial sodium channel (ENaC) by membrane trafficking. *Biochim. Biophys. Acta.* 1802:1166–1177. https://doi.org/10.1016/j.bbadis.2010.03.010

Butterworth, M.B., R.S. Edinger, J.P. Johnson, and R.A. Frizzell. 2005. Acute ENaC stimulation by cAMP in a kidney cell line is mediated by exocytic insertion from a recycling channel pool. *J. Gen. Physiol.* 125:81–101. https://doi.org/10.1085/jgp.200409124

Caldwell, R.A., R.C. Boucher, and M.J. Stutts. 2004. Serine protease activation of near-silent epithelial Na^+ channels. *Am. J. Physiol. Cell Physiol.* 286:C190–C194. https://doi.org/10.1152/ajpcell.00342.2003

Caldwell, R.A., R.C. Boucher, and M.J. Stutts. 2005. Neutrophil elastase activates near-silent epithelial Na^+ channels and increases airway epithelial Na^+ transport. *Am. J. Physiol. Lung Cell. Mol. Physiol.* 288:L813–L819. https://doi.org/10.1152/ajplung.00435.2004

Canessa, C.M., A.M. Merillat, and B.C. Rossier. 1994a. Membrane topology of the epithelial sodium channel in intact cells. *Am. J. Physiol.* 267:C1682–C1690. https://doi.org/10.1152/ajpcell.1994.267.6.C1682

Canessa, C.M., L. Schild, G. Buell, B. Thorens, I. Gautschi, J.D. Horisberger, and B.C. Rossier. 1994b. Amiloride-sensitive epithelial Na^+ channel is made of three homologous subunits. *Nature.* 367:463–467. https://doi.org/10.1038/367463a0

Chalfant, M.L., J.S. Denton, A.L. Langloh, K.H. Karlson, J. Loffing, D.J. Benos, and B.A. Stanton. 1999. The NH_2 terminus of the epithelial sodium channel contains an endocytic motif. *J. Biol. Chem.* 274:32889–32896. https://doi.org/10.1074/jbc.274.46.32889

Cholon, D.M., W.K. O'Neal, S.H. Randell, J.R. Riordan, and M. Gentzsch. 2010. Modulation of endocytic trafficking and apical stability of CFTR in primary human airway epithelial cultures. *Am. J. Physiol. Lung Cell. Mol. Physiol.* 298:L304–L314. https://doi.org/10.1152/ajplung.00016.2009

Chraïbi, A., C. Verdumo, A.M. Mérillat, B.C. Rossier, J.D. Horisberger, and E. Hummler. 2001. Functional analyses of a N-terminal splice variant of the α subunit of the epithelial sodium channel. *Cell. Physiol. Biochem.* 11:115–122. https://doi.org/10.1159/000047799

Diakov, A., K. Bera, M. Mokrushina, B. Krueger, and C. Korbmacher. 2008. Cleavage in the γ-subunit of the epithelial sodium channel (ENaC) plays an important role in the proteolytic activation of near-silent channels. *J. Physiol.* 586:4587–4608. PubMed https://doi.org/https://doi.org/10.1113/jphysiol.2008.154435

Frindt, G., and L.G. Palmer. 2015. Acute effects of aldosterone on the epithelial Na channel in rat kidney. *Am. J. Physiol. Renal Physiol.* 308:F572–F578. https://doi.org/10.1152/ajprenal.00585.2014

Frindt, G., D. Gravotta, and L.G. Palmer. 2016. Regulation of ENaC trafficking in rat kidney. *J. Gen. Physiol.* 147:217–227. https://doi.org/10.1085/jgp.201511533

García-Caballero, A., Y. Dang, H. He, and M.J. Stutts. 2008. ENaC proteolytic regulation by channel-activating protease 2. *J. Gen. Physiol.* 132:521–535. https://doi.org/10.1085/jgp.200810030

Garty, H., and L.G. Palmer. 1997. Epithelial sodium channels: function, structure, and regulation. *Physiol. Rev.* 77:359–396. https://doi.org/10.1152/physrev.1997.77.2.359

Gentzsch, M., H. Dang, Y. Dang, A. Garcia-Caballero, H. Suchindran, R.C. Boucher, and M.J. Stutts. 2010. The cystic fibrosis transmembrane conductance regulator impedes proteolytic stimulation of the epithelial Na^+ channel. *J. Biol. Chem.* 285:32227–32232. https://doi.org/10.1074/jbc.M110.155259

Grieve, A.G., and C. Rabouille. 2011. Golgi bypass: skirting around the heart of classical secretion. *Cold Spring Harb. Perspect. Biol.* 3:a005298. https://doi.org/10.1101/cshperspect.a005298

Heidrich, E., M.D. Carattino, R.P. Hughey, J.M. Pilewski, T.R. Kleyman, and M.M. Myerburg. 2015. Intracellular Na^+ regulates epithelial Na^+ channel maturation. *J. Biol. Chem.* 290:11569–11577. https://doi.org/10.1074/jbc.M115.640763

Hughey, R.P., G.M. Mueller, J.B. Bruns, C.L. Kinlough, P.A. Poland, K.L. Harkleroad, M.D. Carattino, and T.R. Kleyman. 2003. Maturation of the epithelial Na^+ channel involves proteolytic processing of the α- and γ-subunits. *J. Biol. Chem.* 278:37073–37082. https://doi.org/10.1074/jbc.M307003200

Hughey, R.P., J.B. Bruns, C.L. Kinlough, K.L. Harkleroad, Q. Tong, M.D. Carattino, J.P. Johnson, J.D. Stockand, and T.R. Kleyman. 2004a. Epithelial sodium channels are activated by furin-dependent proteolysis. *J. Biol. Chem.* 279:18111–18114. https://doi.org/10.1074/jbc.C400080200

Hughey, R.P., J.B. Bruns, C.L. Kinlough, and T.R. Kleyman. 2004b. Distinct pools of epithelial sodium channels are expressed at the plasma membrane. *J. Biol. Chem.* 279:48491–48494. https://doi.org/10.1074/jbc.C400460200

Kellenberger, S., I. Gautschi, and L. Schild. 2002. An external site controls closing of the epithelial Na^+ channel ENaC. *J. Physiol.* 543:413–424. https://doi.org/10.1113/jphysiol.2002.022020

Kleyman, T.R., M.D. Carattino, and R.P. Hughey. 2009. ENaC at the cutting edge: regulation of epithelial sodium channels by proteases. *J. Biol. Chem.* 284:20447–20451. https://doi.org/10.1074/jbc.R800083200

Knight, K.K., D.M. Wentzlaff, and P.M. Snyder. 2008. Intracellular sodium regulates proteolytic activation of the epithelial sodium channel. *J. Biol. Chem.* 283:27477–27482. https://doi.org/10.1074/jbc.M804176200

Kota, P., A. García-Caballero, H. Dang, M. Gentzsch, M.J. Stutts, and N.V. Dokholyan. 2012. Energetic and structural basis for activation of the epithelial sodium channel by matriptase. *Biochemistry.* 51:3460–3469. https://doi.org/10.1021/bi2014773

Kota, P., G. Buchner, H. Chakraborty, Y.L. Dang, H. He, G.J. Garcia, J. Kubelka, M. Gentzsch, M.J. Stutts, and N.V. Dokholyan. 2014. The N-terminal domain allosterically regulates cleavage and activation of the epithelial sodium channel. *J. Biol. Chem.* 289:23029–23042. https://doi.org/10.1074/jbc.M114.570952

Lippincott-Schwartz, J., L.C. Yuan, J.S. Bonifacino, and R.D. Klausner. 1989. Rapid redistribution of Golgi proteins into the ER in cells treated with brefeldin A: evidence for membrane cycling from Golgi to ER. *Cell.* 56:801–813. https://doi.org/10.1016/0092-8674(89)90685-5

Misumi, Y., Y. Misumi, K. Miki, A. Takatsuki, G. Tamura, and Y. Ikehara. 1986. Novel blockade by brefeldin A of intracellular transport of secretory proteins in cultured rat hepatocytes. *J. Biol. Chem.* 261:11398–11403.

Mueller, G.M., O.B. Kashlan, J.B. Bruns, A.B. Maarouf, M. Aridor, T.R. Kleyman, and R.P. Hughey. 2007. Epithelial sodium channel exit from the endoplasmic reticulum is regulated by a signal within the carboxyl cytoplasmic domain of the α subunit. *J. Biol. Chem.* 282:33475–33483. https://doi.org/10.1074/jbc.M707339200

Myerburg, M.M., M.B. Butterworth, E.E. McKenna, K.W. Peters, R.A. Frizzell, T.R. Kleyman, and J.M. Pilewski. 2006. Airway surface liquid volume regulates ENaC by altering the serine protease-protease inhibitor balance: a mechanism for sodium hyperabsorption in cystic fibrosis. *J. Biol. Chem.* 281:27942–27949. https://doi.org/10.1074/jbc.M606449200

Patel, A.B., G. Frindt, and L.G. Palmer. 2013. Feedback inhibition of ENaC during acute sodium loading in vivo. *Am. J. Physiol. Renal Physiol.* 304:F222–F232. https://doi.org/10.1152/ajprenal.00596.2012

Patel, A.B., L. Yang, S. Deng, and L.G. Palmer. 2014. Feedback inhibition of ENaC: acute and chronic mechanisms. *Channels (Austin).* 8:444–451. https://doi.org/10.4161/19336950.2014.949190

Ruan, Y.C., J.H. Guo, X. Liu, R. Zhang, L.L. Tsang, J.D. Dong, H. Chen, M.K. Yu, X. Jiang, X.H. Zhang, et al. 2012. Activation of the epithelial Na+ channel triggers prostaglandin E_2 release and production required for embryo implantation. *Nat. Med.* 18:1112–1117. https://doi.org/10.1038/nm.2771

Ruffieux-Daidié, D., and O. Staub. 2011. Intracellular ubiquitylation of the epithelial Na^+ channel controls extracellular proteolytic channel activation via conformational change. *J. Biol. Chem.* 286:2416–2424. https://doi.org/10.1074/jbc.M110.176156

Ruffieux-Daidié, D., O. Poirot, S. Boulkroun, F. Verrey, S. Kellenberger, and O. Staub. 2008. Deubiquitylation regulates activation and proteolytic cleavage of ENaC. *J. Am. Soc. Mephrol.* 19:2170–2180. https://doi.org/10.1681/ASN.2007101130

Sheng, S., J. Li, K.A. McNulty, T. Kieber-Emmons, and T.R. Kleyman. 2001. Epithelial sodium channel pore region. structure and role in gating. *J. Biol. Chem.* 276:1326–1334. https://doi.org/10.1074/jbc.M008117200

Snyder, P.M., D.B. Bucher, and D.R. Olson. 2000. Gating induces a conformational change in the outer vestibule of ENaC. *J. Gen. Physiol.* 116:781–790. https://doi.org/10.1085/jgp.116.6.781

Soundararajan, R., M. Lu, and D. Pearce. 2012. Organization of the ENaC-regulatory machinery. *Crit. Rev. Biochem. Mol. Biol.* 47:349–359. https://doi.org/10.3109/10409238.2012.678285

Tarran, R., L. Trout, S.H. Donaldson, and R.C. Boucher. 2006. Soluble mediators, not cilia, determine airway surface liquid volume in normal and cystic fibrosis superficial airway epithelia. *J. Gen. Physiol.* 127:591–604. https://doi.org/10.1085/jgp.200509468

Turnheim, K. 1991. Intrinsic regulation of apical sodium entry in epithelia. *Physiol. Rev.* 71:429–445. https://doi.org/10.1152/physrev.1991.71.2.429

Tveit, H., L.K.A. Akslen, G.L. Fagereng, M.A. Tranulis, and K. Prydz. 2009. A secretory Golgi bypass route to the apical surface domain of epithelial MDCK cells. *Traffic.* 10:1685–1695. https://doi.org/10.1111/j.1600-0854.2009.00984.x

Winarski, K.L., N. Sheng, J. Chen, T.R. Kleyman, and S. Sheng. 2010. Extracellular allosteric regulatory subdomain within the γ subunit of the epithelial Na^+ channel. *J. Biol. Chem.* 285:26088–26096. https://doi.org/10.1074/jbc.M110.149963